Determination of Thermal Load in Film Cooled Bipropellant Thrust Chambers by an Inverse Method

J N Hinckel⋆ and R I Savonov⋆⋆ and H Patire Jr†
⋆Senior Researcher INPE
SJC SP BR
⋆⋆Visiting Researcher - INPE
SJC SP BR
†Researcher INPE
SJC SP BR

Abstract

This paper describes a method to obtain the heat load on the internal wall of a rocket thrust chamber using an inverse problem approach. According to the "classical" approach, the heat load on the internal wall of the chamber is assumed as the product of a heat transfer coefficient and the temperature difference of adiabatic wall temperature and local wall surface temperature. The time dependent temperature distribution of the external wall of the thruster chamber is used to obtain empirical curve fittings to the temperature profile of the near wall flow field (adiabatic wall temperature) and the heat transfer coefficient profile. The applicability of the method is verified by applying it to three different problems; a model problem, an analytical solution, and a set of experimental data.

1. Introduction

The evaluation of the heat load applied to the internal wall of the thrust chamber of rocket engines presents a formidable challenge to the designer of these machines, even for long time practitioners of the art. The analytical tools available for the task are limited by the difficulty of modeling the underlying physical phenomena: the atomization, evaporation, mixing and combustion of the propellants and the flow of the resulting gas mixture.

The discreet nature of the injection process, the minimal chamber volume and the high energy release in the entire volume of the chamber renders meaningless the assumptions of the "classical" analytical solution. Attempts at numerical solution to the problem are also adversely affect by the same problems.

2. Description of the Method

The method described here is intended to be used as a tool to obtain the heat load on the inner surface of the thrust chamber of a rocket engine from the mapping of temperature of the external surface of the chamber. To the degree that the heat load depends only on the flow of the combustion products and that the transient regime of the flow is very short compared to the heating of the chamber wall, data collected during a short test can be used to determine the heat load. In a radiatively cooled chamber the heat load data can be used to evaluate steady state temperature distribution of the chamber for different materials and wall thickness. For heat sink cooled chambers the heat load solution can be used to distribute the heat sinking power along the surface of the wall chamber.

2.1 The Underlying Hypotheses

The basic assumption of this approach is to circumvent the difficulty of direct measurement of the heat load applied to inner surface of the thrust chamber. It is reasonably easy to measure the outside wall temperature and we can model accurately the transfer function relating the convective and radiative heat load applied on the inner wall and a radiating outer wall.

We cannot solve the inverse problem exactly, but, combining our modeling of the conduction transfers across the wall and some reasonable assumptions about the temperature of the combustion products and the gas flow near the wall we can obtain a good estimation of the heat load on the inner wall.

The main hypotheses regarding the temperature of the combustion products and the gas flow near the wall are:

- The characteristic time for the establishment of a steady state flow inside the combustion chamber is much smaller than the time constant for heating of the chamber wall.

- The heat flux from the combustion products to the chamber wall is described with good accuracy by the product of the heat transfer coefficient and the temperature difference between the wall surface and the near wall film temperature (represented by the adiabatic wall temperature).

To the extent that the above hypotheses hold, we can determine the heat load to the thrust chamber with a short test in transient time. The results may be used to extrapolate the wall temperature profile in the steady state. The method may be used to evaluate injector head layouts and chamber geometries (with respect to heat load), using less expensive materials and surface treatment methods to produce thrust chambers capable of operating at very high temperatures.

The method might also be used to evaluate the heat load even in regeneratively cooled chambers. The detailed knowledge of the heat load will help in designing the distribution of the heat sinking profile along the length of the thrust chamber.

2.2 The Governing Equations

The heat load on the internal surface of the chamber wall is given by:

$$q(x, t) = h(x)(T_{aw}(x) - T_w(x, t)) \tag{1}$$

In equation 1 the expressions $h(x)$ and $T_{aw}(x)$ depend only on conditions of the flow inside the chamber and, according to our basic assumptions, depend only on the distance along the axis of the chamber. The characteristic time of these profiles is determined by the combustion process of the propellants.

$T_w(x, t)$ is the temperature of the inner surface of the thrust chamber and depends on the axial coordinate and the time. The temperature of the wall is governed by the transient heat conduction problem with an initial condition of homogeneous temperature distribution, a convective boundary condition on the inside surface and radiative condition on the outside wall. On the inside wall there is also a heat flux due to radiative exchange with the hot gases.

The equations describing this problem are:

$$\nabla[k\nabla T(\mathbf{r}, t)] = \rho C_p \frac{\partial T(\mathbf{r}, t)}{\partial t} \tag{2}$$

The initial condition is:

$$T(\mathbf{r}, t)|_{t=0} = T_0 \tag{3}$$

The boundary condition on the inside wall (without the radiative exchange) is:

$$q(\mathbf{r}, t) = h(\mathbf{r}, t)[T_{aw}(\mathbf{r}) - T_w(\mathbf{r}, t)] \tag{4}$$

The boundary condition on the outside wall is given by:

$$q(\mathbf{r}, t) = \varepsilon\sigma \left\{ [T_w(\mathbf{r}, t)]^4 - T_\infty^4 \right\} \tag{5}$$

2.3 The temperature profile of the near wall flow field

The temperature of the near wall flow film depends on several factors: the amount of fuel injected in the curtain, the heat absorbed by the evaporation and heating of the fuel film, heat lost to the wall and heat released by combustion of the fuel in the film with oxidizer migrating from the core flow. As a result of all these phenomena the temperature of the film is generally increasing from the face of the injector plate towards the exit of the nozzle. The temperature of the film is also limited by two obvious asymptotes; the entrance temperature of the film and the adiabatic wall temperature of the core flow.

A Boltzmann profile curve has the characteristics described above. This curve is described by the following equation;

$$T(x) = \frac{T_1 - T_2}{1 + e^{(x-x_0)/\Delta x}} + T_2 \tag{6}$$

In equation 6 variables T_1 and T_2 are asymptotes, x_0 is the axial coordinate of the mean value of the asymptotes and Δx is the "width" of the growth rate at the x_0 coordinate. By changing the values of these four parameters a large family of curves may be obtained.

2.4 The heat transfer coefficient profile

The heat transfer coefficient profile may be obtained in an approximated form by the Bartz formula. The Bartz formula contains many parameters related to the geometry of the chamber flow profile of the combustion products inside the thrust and thermophysical and transport properties of combustion products. The strongest dependency is with the mass flux which may be expressed via the ratio of the area of the cross section of the chamber in each position along the length of the chamber to the area of the cross section of the chamber at the throat of the nozzle.

The general behavior of the heat transfer coefficient along the length of the chamber is an increase from the injector until the throat and a decrease thereafter.

A type of curve that presents this general behavior is the Lorentz curve described by the following formula:

$$L(x) = \frac{1}{\pi} \frac{\frac{1}{2}\Gamma}{(x - x_0)^2 + \left(\frac{1}{2}\Gamma\right)^2} \tag{7}$$

The Lorentz curve has the following characteristics:
The area under the curve is unitary.

$$\int_{-\infty}^{\infty} L(x) = 1 \tag{8}$$

The function has a maximum at $x = x_0$ given by:

$$L(x_0) = \frac{2}{\pi\Gamma} \tag{9}$$

Γ is the the Full Width at Half Maximum (FWHM).

We redefine the formula so that the horizontal asymptote is H_0 and the maximum is $H_0 + H_1$. To account for the fact that the heat transfer coefficient is not even with respect to the throat axial coordinate, we use two sets of parameters, one for the combustion chamber and subsonic part of the nozzle, $L_l(x)$, and one for the supersonic part of the nozzle, $L_r(x)$.

$$L_l(x) = H_{l_0} + \frac{H_{l_1} W_l^2}{4\left[(x - x_{l_0})^2 + \frac{W_l^2}{4}\right]} \tag{10}$$

and

$$L_r(x) = H_{r_0} + \frac{H_{r_1} W_r^2}{4\left[(x - x_{r_0})^2 + \frac{W_r^2}{4}\right]} \tag{11}$$

The combination of the above equations to form a single profile may done in different ways. The transition occurs near the throat and may be done at a single coordinate point or we can think of a smooth transition over a discrete interval.

We choose a sharp transition at the point x_{l_0}. We further require that the profile be continuous and has no inflexion point near the transition. This condition is satisfied if we set the additional equations for the parameters of the left portion (subsonic) and right portion (supersonic) of the curve $x_{l_0} = x_{r_0} = x_t$ and $H_{r_1} = H_{l_0} + H_{l_1} - H_{r_0}$. This condition reduces by 2 units the number of free parameters of our curve fittings.

(a) Near wall temperature profile for different parameters

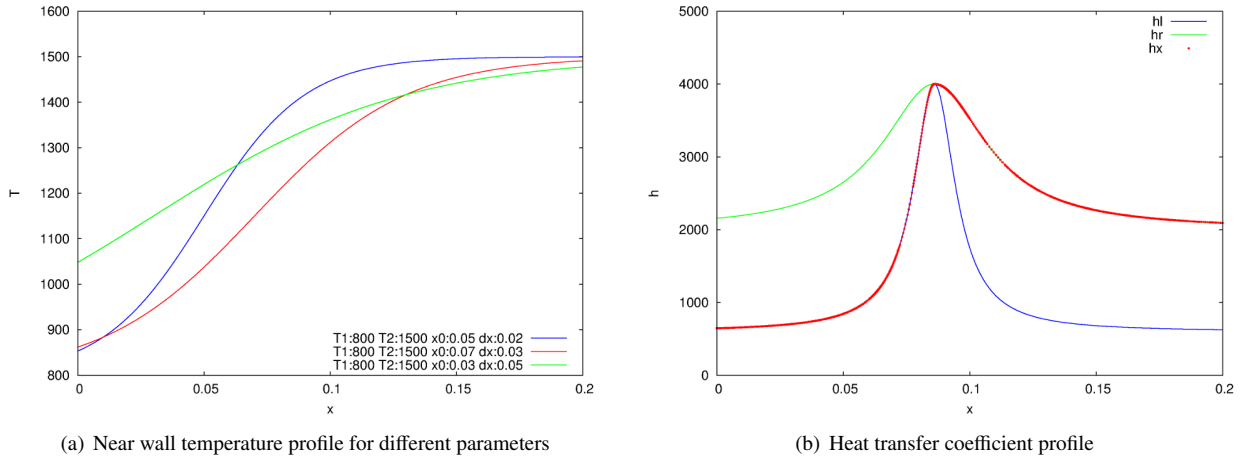

(b) Heat transfer coefficient profile

Figure 1: Boltzmann temperature profile and Lorentz heat transfer coefficient profile

$$h(x) = \begin{cases} L_l(x) & \text{if } x \leq x_t \\ L_r(x) & \text{if } x > x_t \end{cases} \tag{12}$$

Figure 1 shows the Boltzmann type temperature profile for the near wall film, and the Lorentz type heat transfer coefficient profile. This family of curves is large but limited, and certainly does not constitute a base space for all possible profiles.

3. The algorithm

Equations 6 and 12 define the thermal load on the inner surface of the thrust chamber. The 10 free parameters of the heat load are determined by minimizing the difference between the measured temperature on the outside surface of the wall and the temperature profile obtained from the solution of the transient heat conduction in the wall with the applied heat load.

The transient heat conduction problem for the thrust chamber wall is solved numerically using a finite element based application.

The "merit function" to be minimized is given by:

$$\chi^2(\mathbf{a}) = \sum_{i=1}^{N} \left[y_i - y(x_i; \mathbf{a}) \right]^2 \tag{13}$$

where y_i is the vector of the measured temperature values along the external surface and $y(x_i; \mathbf{a})$ is the vector of temperature values at the corresponding points obtained from the "test" heat load. In the solution presented here, the merit function is evaluated at one single time point during the transient or in the steady state. We could also define the merit function based on the difference of the temperatures summed over different time intervals.

Vector $\mathbf{a}$ is defined by:

$$\mathbf{a} = \{T1, T2, x_0, \Delta x, H_{l_0}, H_{l_1}, x_t, W_l, H_{r_0}, W_r\} \tag{14}$$

The algorithm due to Marquardt, usually referred to as the Levenberg-Marquardt method, described in [4], is used in the iterative process to obtain vector $\mathbf{a}$.

4. Validation

The validation of the method was done in various steps.

4.1 The model problem

In the first step the method was verified for consistency. A set of "reasonable" values of the heat load parameters was assumed (i.e.; we populated the vector **a**.). With this "reasonable" heat load the transient heat conduction problem in the chamber wall was solved and the temperature profile on the external wall surface was obtained in several steps during the transient heating of the wall and in the steady state. The initial condition was homogeneous temperature. External surface boundary condition was radiation to empty medium. These data were fed into the method to recover the heat load parameters.

The whole sequence of jobs is as follows:

- Chose a value of vector **a**.

- Solve problem for transient time and steady-state.

- Compare capability of method to capture initial values of vector **a** in the transient time and in steady state.

Two wall geometries were used. In the first geometry the wall thickness was uniform. As the thickness of the wall decreases the axial conduction along the wall can be neglected and the heat resistance is due only to the convection and radiation. In the second geometry the wall thickness of the thrust chamber varies along the length of the chamber .The geometries of the chamber are presented in Figure 2. The thickness of the uniform wall was 1 mm. The thickness of the variable wall varied from 1 to 6 mm. The material thermophysical properties used in the solution were those of Inconel 600.
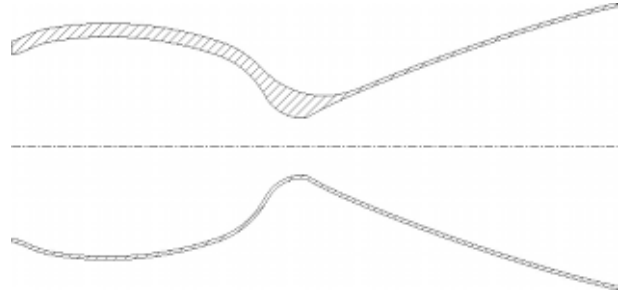
The convergence of the iterative process is sensitive to the "closeness" of the guess vector. If the guess vector is to far off the solution, the iterative process may

Figure 2: Wall chamber geometry

not converge at all. When convergence is achieved the number of iterations is in the range of 20 to 100, depending on the desired accuracy and closeness of the guess vector to the solution. It should be noted that in this model problem the imposed heat load profile matches the fitting curves. Therefore, an exact value of the solution exits and, in principle, may be obtained.

As expected, the algorithm was able to recover the heat load data with great accuracy. The results for the two geometries are shown in Table 4.1. The external wall temperature profile for the reference data and recovered data are in very good agreement except for the case of the variable wall thickness with reference data from the interval of 1 second in the transient heating of the wall.

The external surface temperature calculated for the reference heat load and the recovered data heat load is shown in Figure 3. The surface temperature is plotted for the two geometries during the transient time in the intervals of 1 s

Table 1: Values of reference vector and recovered vector; in steady state and during transient

	$T1$	$T2$	x_0	Δx	H_{l_0}	H_{l_1}	x_t	W_l	H_{r_0}	H_{r_1}	W_r
Reference	800	1500	0.05	0.02	600	3400	0.086	0.02		3500	0.05
Guess	550	2000	0.035	0.014	780	4000	0.09	0.026	280	4500	0.065
Uniform wall thickness											
Recovered: SS	800	1500	0.05	0.02	598.4	3388	0.0862	0.02	498	3488	0.05
Recovered: 5s	800.4	1499.4	0.05	0.02	599	3407	0.0862	0.02	501	3505	0.05
Recovered: 1s	800	1500	0.05	0.02	600	3397	0.0862	0.02	499	3498	0.05
Variable wall thickness											
Recovered: SS	800	1500	0.05	0.02	600.4	3400.4	0.0862	0.02	500	3500	0.05
Recovered: 5s	800	1500	0.05	0.02	600	3400	0.0862	0.02	500	3500	0.05
Recovered: 1s	690.4	1606	0.065	0.026	727	3627	0.0862	0.021	446	3908	0.046

(a) External wall temperature; uniform wall thickness

(b) External wall temperature; variable wall thickness
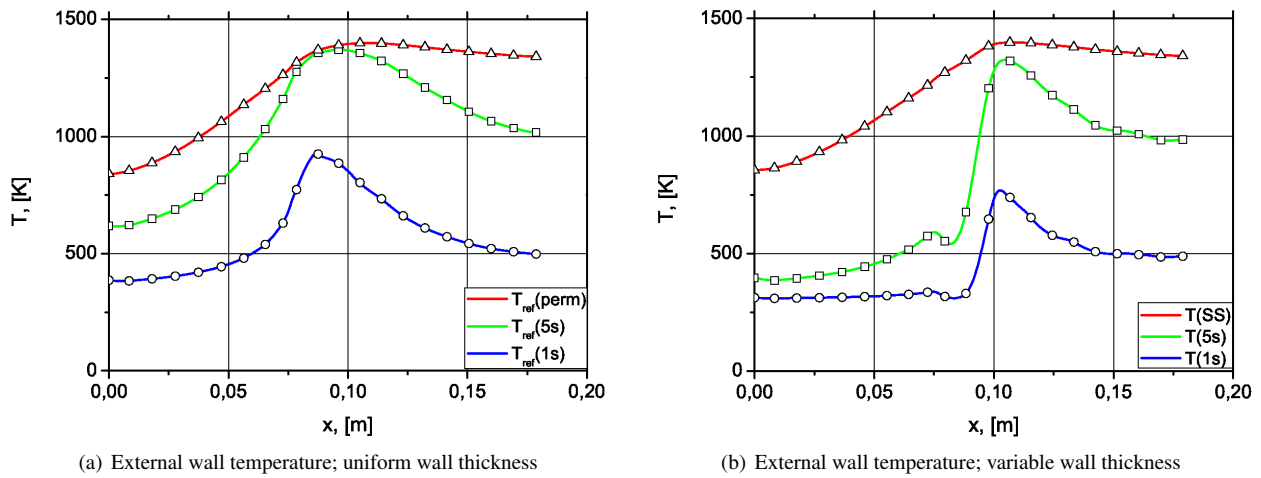
Figure 3: External surface temperature from reference data and recovered data: two geometries, transient time and steady state

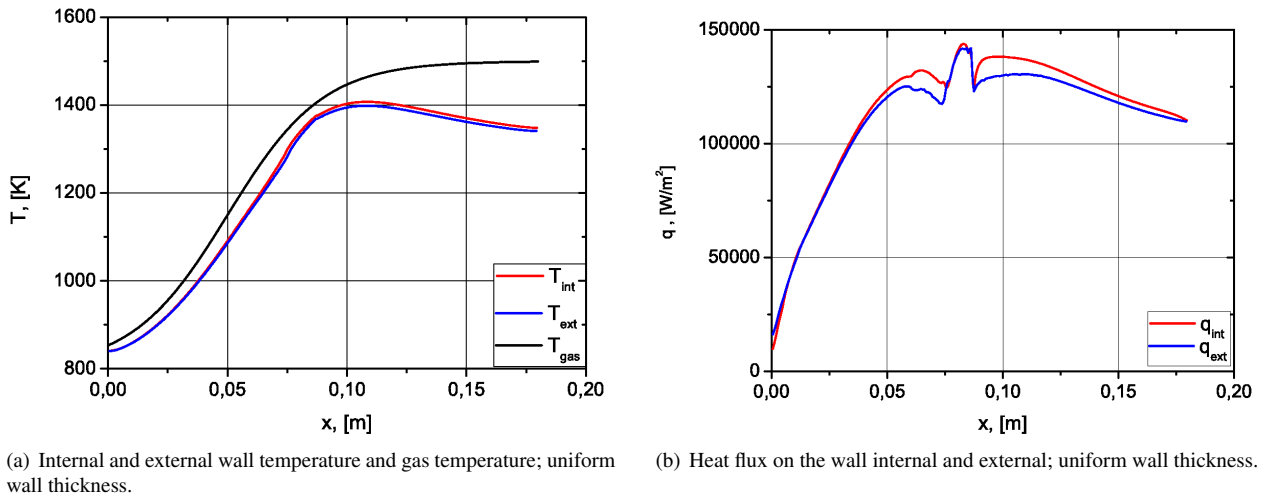(a) Internal and external wall temperature and gas temperature; uniform wall thickness.

(b) Heat flux on the wall internal and external; uniform wall thickness.

Figure 4: Adiabatic wall temperature, internal and external wall temperature and internal and external wall heat flux. Steady state condition

and 5 s, and in the steady state. Each curve is composed of a continuous line and supper-imposed staggered symbols. The continuous line refers to the reference heat load condition. The staggered symbol curve refers to the recovered heat load data.

It is interesting to note that even for the case of the variable wall thickness in the 1 second interval transient condition, there is a very good agreement between the curves for the reference heat load and the recovered data heat load. This suggests that our profiles for the heat transfer coefficient and the temperature difference are not "orthogonal" under this conditions.

In Figure 4 we show the near wall gas temperature profile, the internal and external wall surface temperature profile and the heat flux on the internal and external wall surface. These data refer to the uniform wall thickness chamber in the steady state.

4.2 The Bartz solution

In the second step, the temperature profile of the near wall flow field was assumed to be given by the stagnation temperature of the combustion product, corrected along the length of the chamber by the recovery factor. The heat transfer coefficient was calculated by the Bartz formula. A description of the Bartz method is presented in [3] and [2].
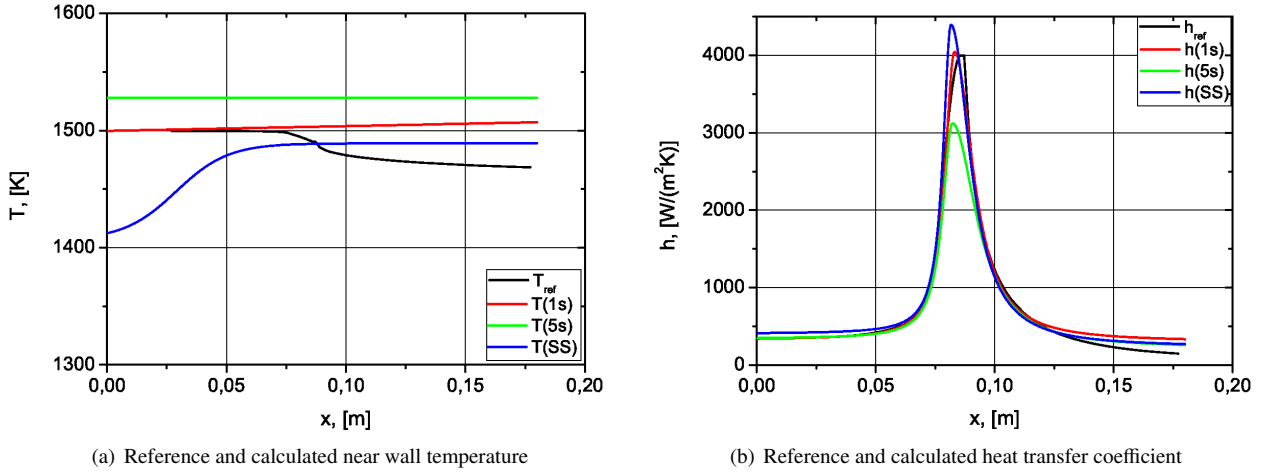
(a) Reference and calculated near wall temperature

(b) Reference and calculated heat transfer coefficient

Figure 5: Boltzmann and Lorentz fitting for the Bartz heat load. Uniform wall thickness thrust chamber

(a) Reference and calculated near wall temperature
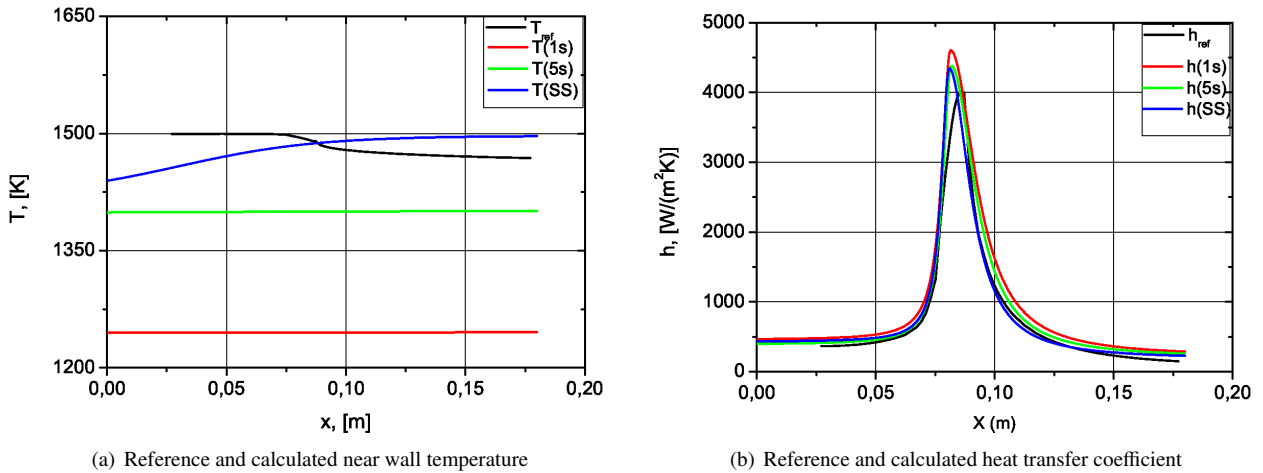
(b) Reference and calculated heat transfer coefficient

Figure 6: Boltzmann and Lorentz fittings for the Bartz heat load. Variable wall thickness thrust chamber

The purpose of this step was to show that the chosen near wall temperature profile and heat transfer coefficient profile could represent reasonably well "real world" conditions.

The fittings obtained for the near wall flow field temperature and the heat transfer coefficient for the Bartz heat load and a uniform thickness thrust chamber are shown in Figure 5. Figure 6 shows the fittings for the variable wall thickness thrust chamber.

The agreement between the reference Bartz heat transfer coefficient profile and the Lorentz fitting is good. In the initial calculations the merit function was evaluated using the temperature and heat transfer coefficient profiles along the whole length of thrust chamber. Under theses conditions the convergence of the method was poor and value of our merit function at the end of the iterative process was very high. The main reason for this is that the Boltzmann and Lorentz families of fittings are not a "complete base" for the representation of the heat load.

Unlike the model problem, the imposed heat load is not guaranteed to have a profile that can be matched exactly by our fitting curves. Convergence to an exact solution is therefore not usually expected.

To improve results in the region of high heat transfer rate we clipped the domain of the evaluation of the merit function. The temperature data for the initial length of chamber and the final part of the expansion nozzle were dropped from the calculation of the merit function.

The results for the near wall film temperature (adiabatic wall temperature) were also in good agreement with the reference temperature. The results improved as the test time during the transient increased. The best results are those for the steady state.

Even though the Boltzmann fitting would be able to represent the decreasing profile of the reference temperature,

(a) External wall temperature; uniform wall thickness

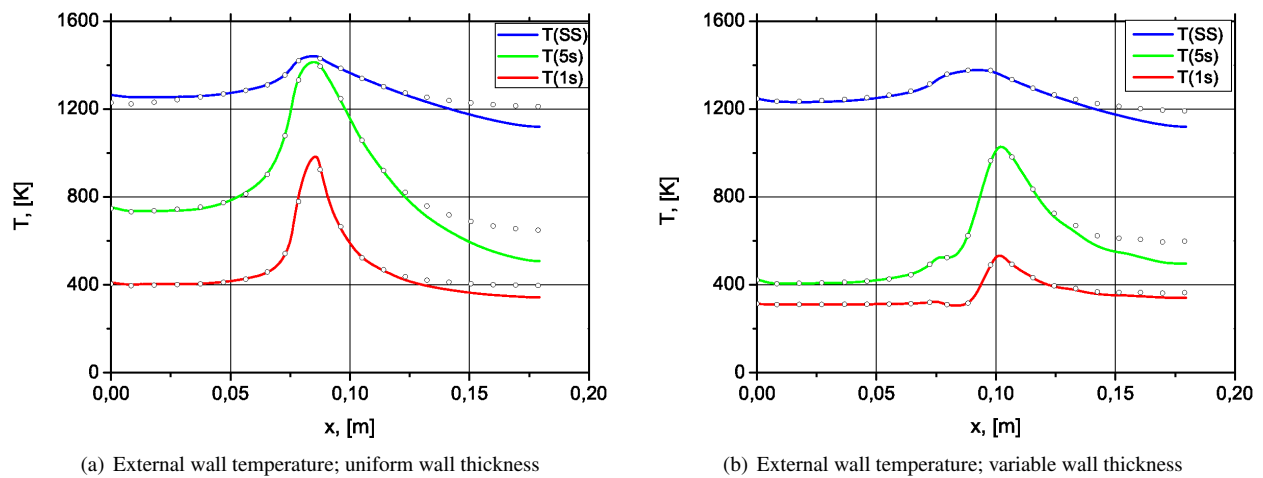(b) External wall temperature; variable wall thickness

Figure 7: External wall temperature. Bartz reference curves and fitting curves

the recovered temperature profile was increasing along the length of the chamber.

The reference external temperature profile and fitted data temperature profiles are shown in Figure 7.

The effects of the data clipping in the evaluation of the merit function are evident in the external wall temperature figures. Agreement between reference data and recovered data is better in the central part of the chamber; in the initial part of the chamber and near the end of the nozzle the values of the temperature for the two sets of data are considerably different.

4.3 Experimental data

In the third step "real experimental data" obtained from fire tests of a 400 N bipropellant thruster were used to calculate the heat load.

The experimental data were obtained from a 400 N bipropellant engine. The propellant pair is the NTO/MMH (Nitrogen Tetroxide / Mono methyl Hydrazine). The test had a duration of 15 seconds. The engine was tested with mixture ratio in the range of 1.0:1 to 1.4:1. The data used for the analysis presented here were obtained from a test with mixture ratio of 1.1:1. The engine geometry and head construction are presented in [1]. The wall geometry is the variable wall thickness of Figure 2.

The external wall temperature was recorded with an FLIR SYSTEMS infrared camera Model ThermaCAM SC3000. The maximum rate of recording is 30 frames per second with a grid of 320 X 240 pixels.

Color coded pictures of the infrared images in three time intervals during the test are shown in Figure 8

The distance between the viewing port and the thrust chamber was approximately 1.5 m.

The camera was mounted outside the test chamber. The data were collected across a glass viewing port. Calibration of the camera was carried out in the following way.

First the thrust chamber was mounted at a distance of 1.5m in direct view sight of camera. The thrust chamber was heated by a gas blowing heat gun to temperature up to 150°C · The readings of two thermocouples attached to the thrust chamber near view sight were used as reference value for the temperature. The emissivity parameter of data processing unit of the camera was adjusted so that the temperature obtained by the camera was equal to the reference temperature from the thermocouple readings.

Next the thrust chamber was mounted inside the vacuum chamber and the temperature data were taken with the infrared camera looking across the glass viewing port. The transmissivity (of the glass viewing port) parameter of the data processing software was adjusted.

The measured data were taken in 41 points equally distributed along the length of the chamber. At each position the value of the temperature was averaged over an arc of approximately 30°, centered on the axis of the chamber.

The fittings obtained for the near wall flow field temperature and the heat transfer coefficient for the experimental heat load are shown in Figure 9. The fittings were obtained from the wall temperature data in three time intervals; 5 s , 10 s and 15 s ·

As with the Bartz model problem, the temperature data were clipped to a region near the throat of chamber.
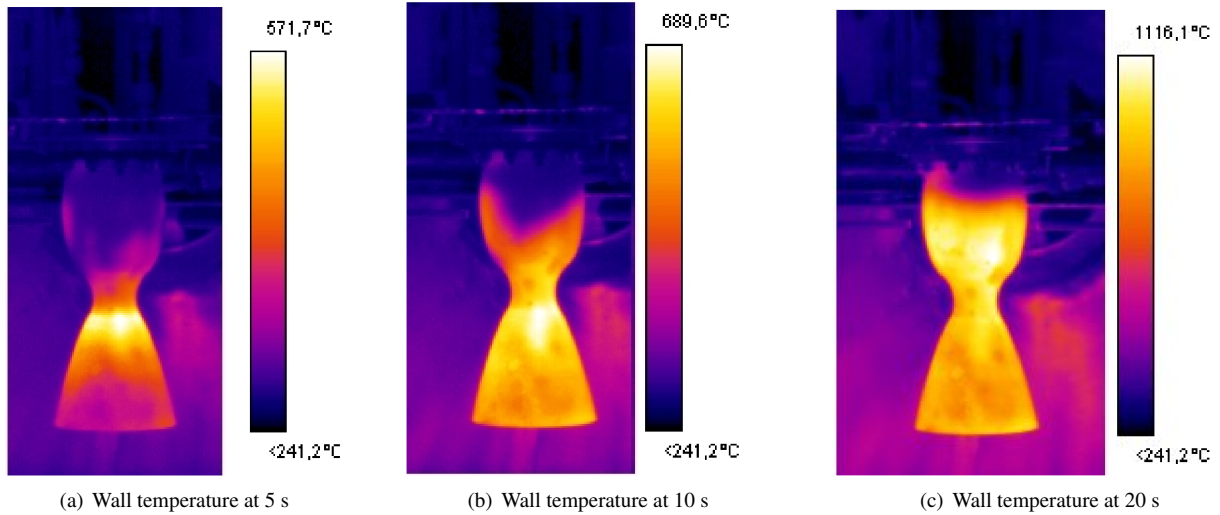
(a) Wall temperature at 5 s   (b) Wall temperature at 10 s   (c) Wall temperature at 20 s

Figure 8: Color coded infrared images of the thruster chamber wall temperature

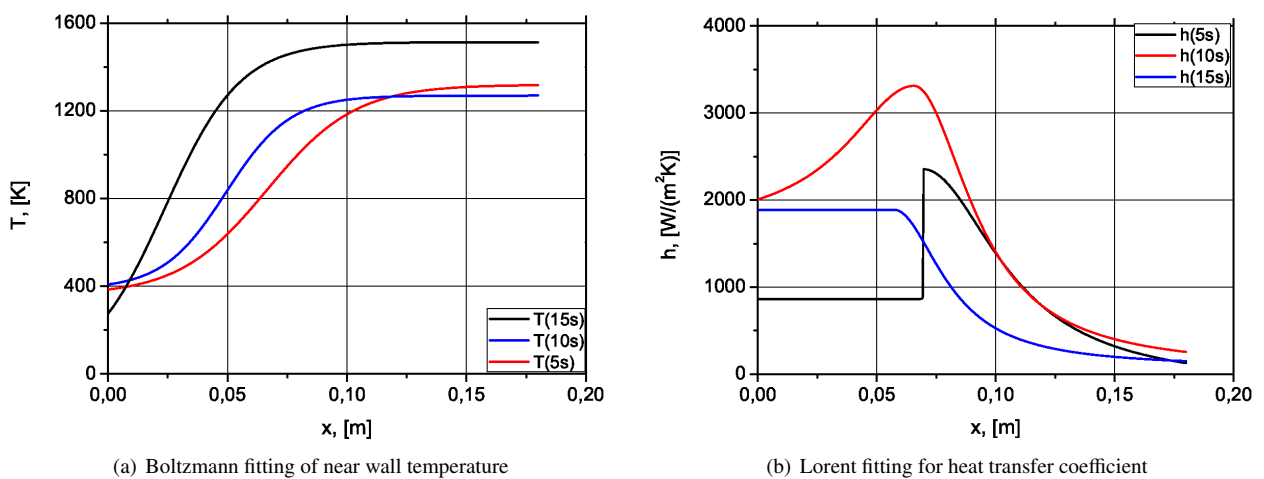(a) Boltzmann fitting of near wall temperature   (b) Lorent fitting for heat transfer coefficient

Figure 9: Boltzmann and Lorentz fittings for the experimental heat load. Niobium variable wall thickness thrust chamber

(a) Experimental temperature data and recovered data: experimental

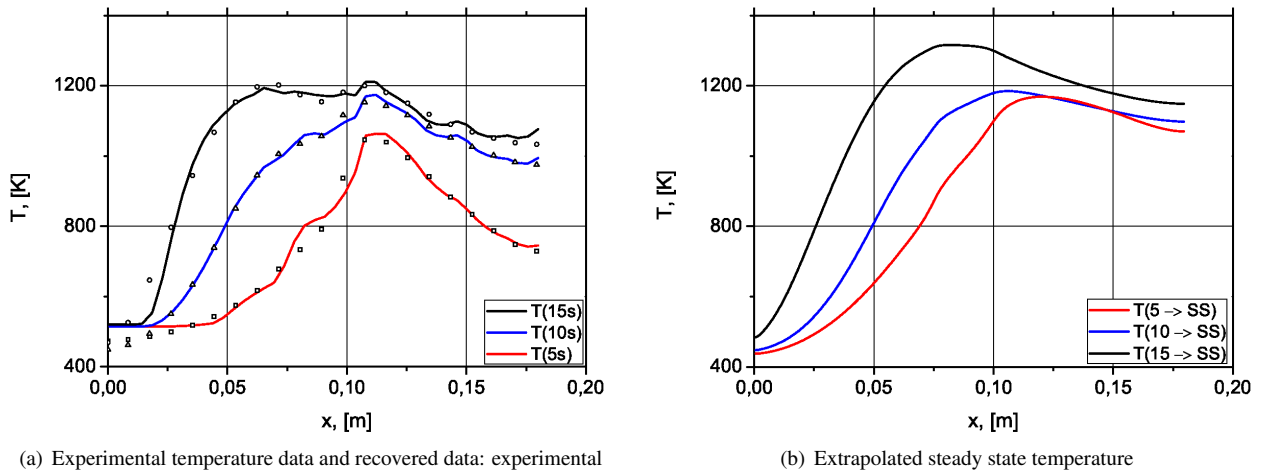(b) Extrapolated steady state temperature

Figure 10: Surface temperature data, fittings data and extrapolation to steady state

The Boltzmann temperature profile has the increasing value along the length of thrust chamber as expected. The lower value of the temperature is approximately the same, but the upper value obtained from the 15 s data is approximately 250°C higher than the value obtained from the data of 5 s and 10 s · It is apparent that with increasing time of test the point of maximum increase of the near wall gas temperature moves closer to the injector face of the engine.

The discrepancy in the Lorentz heat transfer coefficient profile was more pronounced. The maximum value was located near the throat, but the magnitude of the value varied by up to 50%. Only the data from the 10 s interval yielded a curve with a smooth maximum in the throat region. For the 5 s and 15 s interval the heat transfer coefficient upstream of the throat was constant.

The behavior of both the Boltzmann fitting and the Lorentz fitting point to a conclusion that the heat load in the thrust chamber upstream of the throat region increases with time.

Figure 10(a) shows the experimental surface temperature data and the temperature profile obtained by the equivalent heat load. For each time interval there is a very good agreement between both sets of values.

Figure 10(b) shows the steady state external wall temperature profile projected from the heat loads determined in three time intervals. The projected steady state temperature of the supersonic part of the nozzle is very close for the heat load obtained in the three time intervals. In the combustion chamber and subsonic part of the nozzle, the projected steady state temperature increases with increasing time interval of the data used to obtain the heat load.

This behavior contradicts our assumption that the the heat load does not change with time. One possible reason is that the heating of the wall accelerates the evaporation of the fuel film near the wall and the reaction front moves upstream. It is also important to note that the heat load on the wall due to radiation of the combustion products is not included in our calculations and this effect is more pronounced in the region upstream from the throat.

With respect to the experimental data used in the analysis it must be observed that the axial symmetry of the heat load is poor. In the same axial position there are azimuthal variation of the surface temperature and therefore of heat load. this variation is not included in the solution of the heat conduction problem.

Figure 11 shows the measured temperature profile in two time intervals and the cross projected temperature profile from heat load measured in the other time intervals. The time increasing heat load on the wall upstream from the throat is also evident in this Figure.

5. Conclusion

A method to "see through" the thruster wall chamber using an inverse problem formulation is described. The method yields the heat load on the internal surface of the wall from the temperature measurement on the outside surface of the chamber.

A Boltzmann fitting is used to describe the temperature profile of the near wall gas flow temperature (adiabatic wall temperature). A Lorentz fitting is used to describe the heat transfer coefficient profile along the length of the thrust chamber.
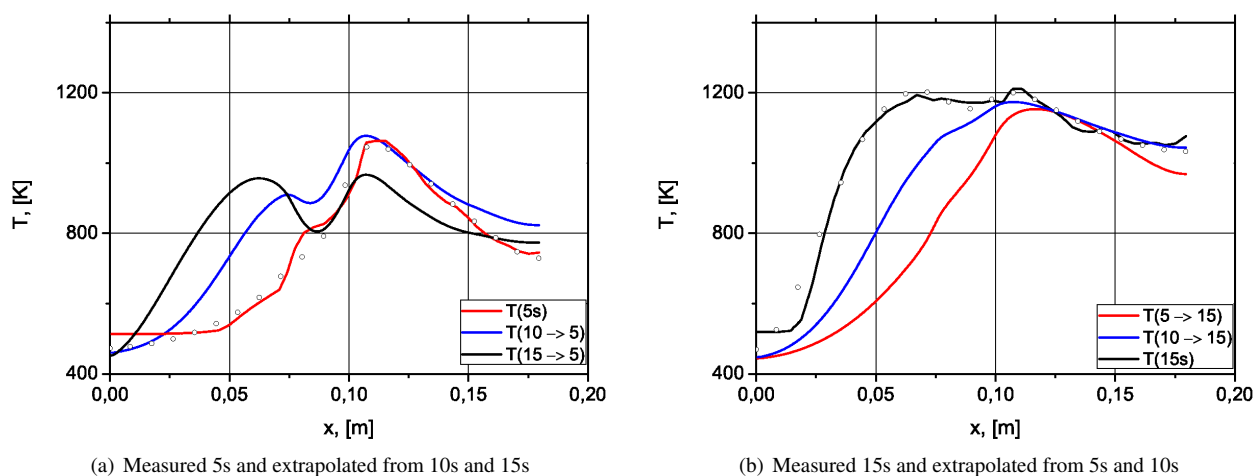
(a) Measured 5s and extrapolated from 10s and 15s

(b) Measured 15s and extrapolated from 5s and 10s

Figure 11: Surface temperature and cross extrapolation

A model problems is used to verify the self-consistency of the algorithm employed to obtain the fittings.

The analytical solution due to Bartz is used to test the capability of the curve fittings to capture the expected profile of the heat load along the length of the thrust chamber.

The experimental validation of the method is done by using test data from fire test of a 400 N bipropellant engine. The test engines uses a swirl injector head plate and a radiation cooled thrust chamber.

The analysis of the data obtained suggests a time increasing heat load upstream of the chamber nozzle throat.

For further improvement of the method, curve fittings with better "base completeness and "orthogonality" characteristics are desirable.

The accuracy of the experimental data, especially in the high range temperature is also needed to improve the confidence in the results of the analysis.

References

[1] 4th European Conference for Aerospace Sciences. *A 400 N bipropellant thruster with swirl injectors*, number Eucass 2011-563, Saint Petersburg, July, 4-8 2011.

[2] P. G. Hill and C. R. Peterson. *Mechanics and Termodynamics of Propulsion*. Addison Wesley Publishing Company, Reading, MA, USA, 1970.

[3] D. K. Huzel and D. H. Huang. *Modern Engineering for Design of Liquid-Propellant Rocket Engines*. American Institute of Aeronautics and Astronautics, Washington DC, USA, 1992.

[4] W. H. Press, S. A. Teukolsky, W. T. Vetterling, and B. P. Flannery. *Numerical Recipes in C*. Cambridge University Press, second edition, 1999.